



# Linear LED driver design and its implementation for visible light communication applications



Syifaул Fuada<sup>a,\*</sup>, Faisal Ahmed<sup>b</sup>, Trio Adiono<sup>c</sup>, Adisorn Kaewpukdee<sup>d</sup>,  
Vita Awalia Mardiana<sup>e</sup>

<sup>a</sup> Program Studi Sistem Telekomunikasi, Universitas Pendidikan Indonesia, Indonesia

<sup>b</sup> Center for Sensor Systems (ZESS), University of Siegen, Germany

<sup>c</sup> University Center of Excellence on Microelectronics, Institut Teknologi Bandung, Indonesia

<sup>d</sup> Department of Electrical Engineering, Faculty of Science and Technology, Nakhon Pathom Rajabhat University, Thailand

<sup>e</sup> Electronics and Telecommunication Research Center, National Research and Innovation Agency of Republik of Indonesia (BRIN), Indonesia

## ARTICLE INFO

### Keywords:

Linear LED Driver  
Bias-T  
Op-Amp  
Visible light communication

## ABSTRACT

This study aimed to develop a linear LED driver for VLC applications which is capable of transmitting multilevel amplitude, such as OFDM formats or pure analog audio – video signals. The proposed driver comprises a general Op-Amp circuit that emits 3–12 Watts LED power. The maximum current of an Op-Amp limits the LED power. This study characterizing the I-V curves and provide insights on how to attain the LED suitable or optimal biasing point. First, the information signal undergoes clipping due to the too high bias point. Second, the LED cannot light up because the bias point is too low. Differently from the conventional Bias-T LED drivers, we exploited the readily available components such as Op-Amp that allows to work as adder device between the data signal and the DC offset. It is also a cost-effective way that uses off-the-shelf Op-Amps. Furthermore, the driver incorporates a DC-offset remover capability for an input similar to the DC signal. The experimental results showed that the linear driver's bandwidth (BW) is  $\geq 500$  kHz without affecting the LED when lighting up. Moreover, the design was evaluated with BER analysis and demonstrated with a real VLC transceiver platform. The transceiver platform comprises FPGA Zync-7000, AD7302 DAC, XADC, and an off-the-shelf Analog Front-End (AFE) receiver. The proposed linear driver was clocked at 100 kHz to perform real-time VLC transmission using QPSK modulation and maximum bit-rate measurement. We have achieved a BER of  $< 1.5 \times 10^{-3}$  and  $\sim 30$  kbps of real-time transmission speed. Therefore, it has a huge potential in IoT-based VLC networks.

## 1. Introduction

Visible Light Communication (VLC) was developed from optical wireless communication (OWC) that utilizes 380–780 nm visible light spectrum as an information transmission medium currently still strategic in the optical field. The pioneer VLC work was initially demonstrated at the Nakagawa Laboratory, Keio University, Japan [1], using a white LED as an antenna device. Due to its outstanding prospects, a VLC Consortium (VLCC) was formed and contributed to developing three VLC standards [2]. The standards include

\* Corresponding author.

E-mail address: [syifaulfuada@upi.edu](mailto:syifaulfuada@upi.edu) (S. Fuada).

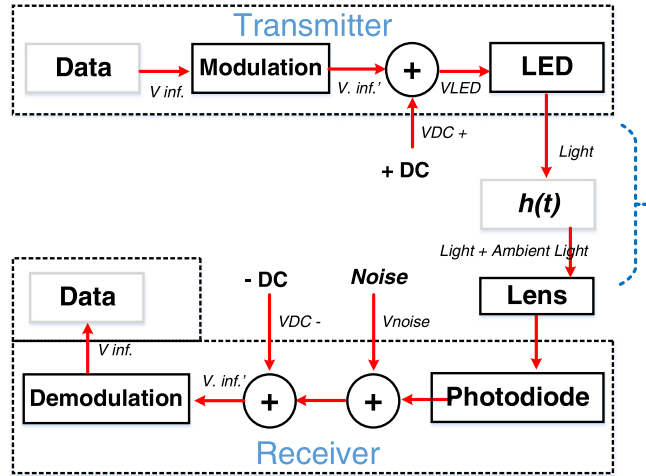


Fig. 1. VLC system modelling reproduced from [6,7].

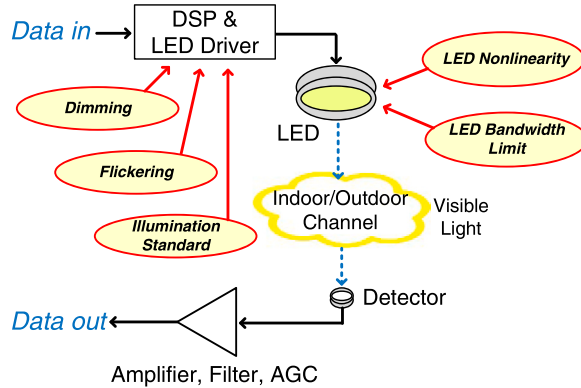


Fig. 2. Issues on the VLC transmitter section, reproduced from [8].

CP-1221 for general visible light communication, CP-1222 for identification system (ID) published in 2007, and CP-1223 for a beacon communication system in 2013. IEEE 802.15.7 is a more comprehensive VLC standard used as a reference for global studies. It comprises the physical (PHY) and MAC layers with the proposed three modulations.

The underlying principle of VL communication is shown in Fig. 1. The signal is then fed to the analog modulator circuit to convert the electrical into the optical signal via the LED. The binary data signals are represented by means of "1" as high and 0 with low voltage levels. These levels allow to control the LED illumination brightness on transmitter front. Furthermore, on the detection side, photodiode receives optical power linearly to the illumination level. LED emits high power signals at short that cover long distance between emitter and receiver. As a result, photodiode receives more power due to direct link phenomenon.

Photodiode is used to convert the optical signal into the electric current [3]. The trans-impedance amplifier (TIA) circuit converts photodiode current ( $i_{PD}$ ) into voltage ( $V_{TIA}$ ) for processing in the following circuit [4]. State-of-the-art VLC drivers are still afflicted by number of bottlenecks in designing VLC systems, which generally use a transistor and Op-Amp configurations, photodiodes, and LED from the local market [5]. Practitioner should revisit the designing processes in accordance to the main problems while developing the VLC systems; this includes considerations in combining these components to objectify the VLC prototype.

Related works have summarized number of challenges and problems which are associated with the VLC transmitters as demonstrated in Fig. 2. These include a) Flicker effect caused by too low input frequency, b) Dimming effect of too high input frequency and improper duty cycle setting, c) Indoor or outdoor lighting standards when the infrastructure is used for multiple functions, d) LED nonlinear factor, and e) LED bandwidth (BW) that can reach up to a few tens of MHz.

The LED driver is part of the transmitter block that modulates the emitted light signals. This ensures no dimming and flickering effect and compensates for the LED nonlinear factor. It is important to consider the exploited modulation while designing the driving circuits. Mostly single carriers are exploited for digital signals, such as on-off keying (OOK), Pulse Position Modulation (PPM), and Pulse Width Modulation (PWM). These aforementioned modulations are easier to implement due to inherent features of amplitude level that conditioned based on '0' or '1' signal levels. Therefore, the LED driver controls by switching on and off mode. Figs. 3 and 4 are the control circuit say it explicitly and threshold setting, respectively. The only difference between OOK, PWM, and PPM is the pulse

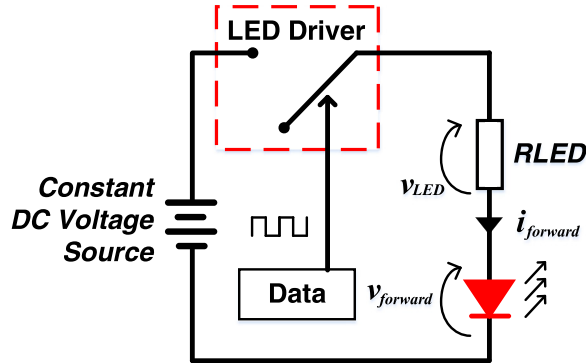


**Fig. 3.** The basic block of control circuits when using constant amplitude digital modulation, which is adopted from [4].

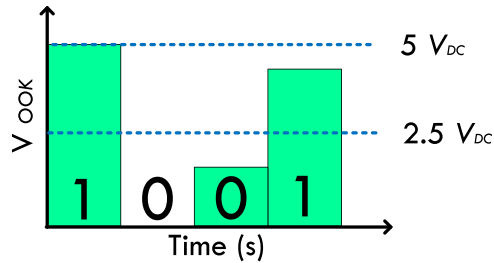


**Fig. 4.** Brightness level setting on the LED uses OOK digital modulation on ARDUINO when using  $5 V_{DC}$  voltage, where voltage  $> 2.5 V_{DC}$  is considered "1" and  $< 2.5 V_{DC}$  is considered "0".

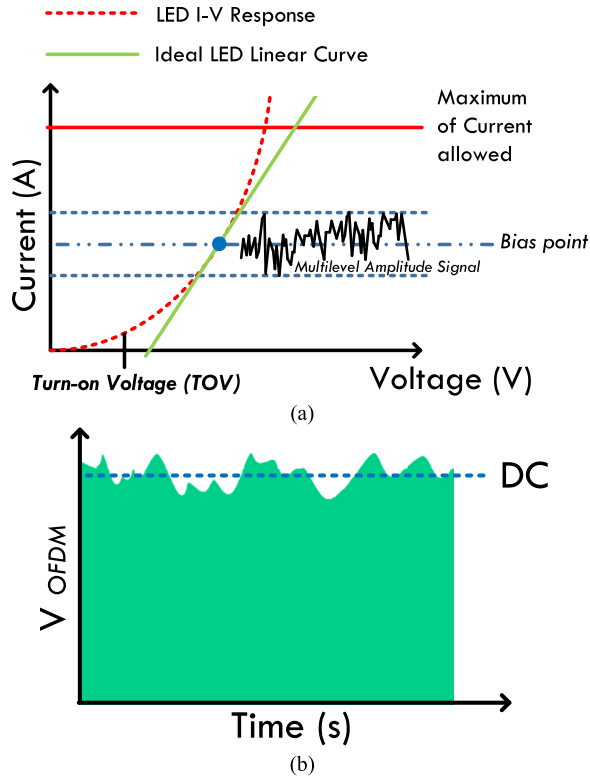


**Fig. 5.** Nonlinear characteristics of LEDs for OFDM: (a) proper bias point setting procedure, reproduced from [18]; (b) Typical OFDM signal on a VLC system, reproduced from [4].

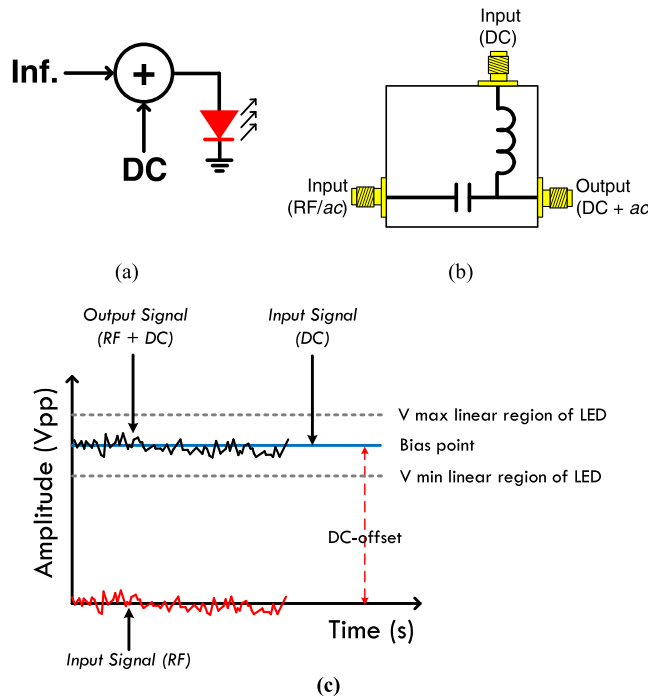


**Fig. 6.** Linear LED driver; (a) analog modulator modeling; (b) the basic topology of the Bias-T module consisting of L & C components, as well as the form of commercial products (Aeroflex® from Apitech corp. taken from [20] & from SVP Broadcast microwave, taken from [21]; (c) working principle of Bias-T module.

width setting. A previous study performed a simple LED driver performance demonstration for OOK modulation using a single transistor and a resistor component for biasing, referring to the block in Fig. 2 [9]. Signal characteristics with multilevel amplitude, such as audio and video signal, and modified OFDM for VLC, including DCO-OFDM and ACO-OFDM, cannot be performed by setting the LED driver to an on-to-off mode or vice versa; this is due to the nonlinear property of LED sources, as reported in [10], which is one the challenging problem in existing literature. To this end, we proposed a driver circuit which is an analog modulator. This maintains the signal in the linear range by avoiding distortion due to the clipping. Furthermore, the inappropriate setting of the information signal's amplitude level causes a flicker effect that interferes with the lighting function and endangers human eye health [11–13].

OOK and PPM modulation are more resistant to LED nonlinearity. Unfortunately, these modulations can not be used for high-speed application due to the inefficient use of BW [14]. Amplitude multilevel characteristic modulation is used before designing the LED driver. However, the forward bias voltage curve against the forward current should be well comprehended. The designer should determine the bias point accurately [15–17]. Fig. 5(a) shows the bias point in which its determination is important in designing a linear LED driver [4]. The designer should design a driver circuit that can perform dual functions without affecting its main role of illumination and now with additional communication services. An illustration of the OFDM signal characteristics in Fig. 5(b) differs from Fig. 4 based on the OOK signal.

In Fig. 5, the LED voltage is the sum of the OFDM or information and DC signals, described mathematically as  $V_{LED} = V_{information} + V_{DC}$ . Fig. 6(a) shows the system illustration. Bias-T is a radio frequency (RF) communication system module widely adopted as an analog modulator in OFDM-based VLC systems. It offers a lightweight implementation and is available in the market with varying BW, from hundreds to thousands of Hertz (Hz). The module is called a “tee” because the basic circuit has three ports arranged to form the letter “T.” These are two inputs or channels for RF and DC signals and one output or the sum of RF and DC signals. The Bias-T module adds a high RF or an information signal with a DC signal, as demonstrated in Fig. 6(b).

Capacitor (C) blocks the DC signal from the power supply and passes the information signal. The inductor (L) blocks AC signals and passes DC signals [19–21]. Therefore, the T-Bias module's output is a mix between the information and the DC signals. In this case, signals with multilevel amplitude characteristics such as OFDM are easily clipped to the LED's linear region via DC voltage adjustment. Fig. 6(c) illustrates the T-Bias operation. The module is relatively expensive [17,22], making it less appropriate for mass OFDM-based VLC installations in commercial buildings, though it could be used for communication with high data rates up to the Gbps range. Therefore, an alternative solution is needed to replace the function of this module.

Previous studies proposed a linear LED driver using Op-Amp circuits comprising a buffer configuration with a summing amplifier. The design was more affordable and worked with a principle similar to Fig. 6(c). The proposed design of LED linear driver BW is  $\sim 1$  MHz and 500 kHz. This can be used for LEDs with power  $> 5$  Watt and compensates for DC-offset input signals. Previous studies also demonstrated the transmission of audio signals via visible light with the same linear LED driver design [6], and also internet data [23]. The transceiver circuit's bit-error-rate (BER) was not investigated because this study was only focused on functional tests.

**Table 1**  
Specifications of Op-Amp TL072.

| IC    | GBW (MHz) | Supply Max. (V <sub>DC</sub> ) | V <sub>out</sub> Max. (V <sub>DC</sub> ) | Features                    |
|-------|-----------|--------------------------------|--|-----------------------------|
| TL072 | 3         | ±18                            | 12                                       | Low-noise JFET-Input Op-Amp |

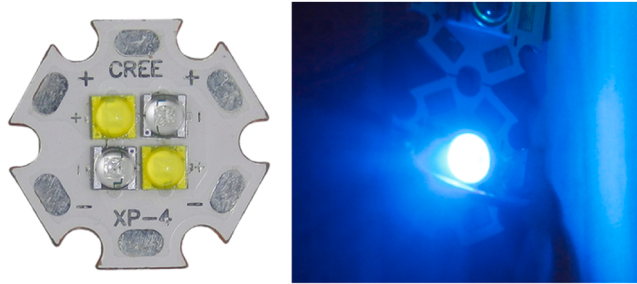


Fig. 7. Pictural view of Blue LED XTE CREE ( $V_{DC}=12$  V).

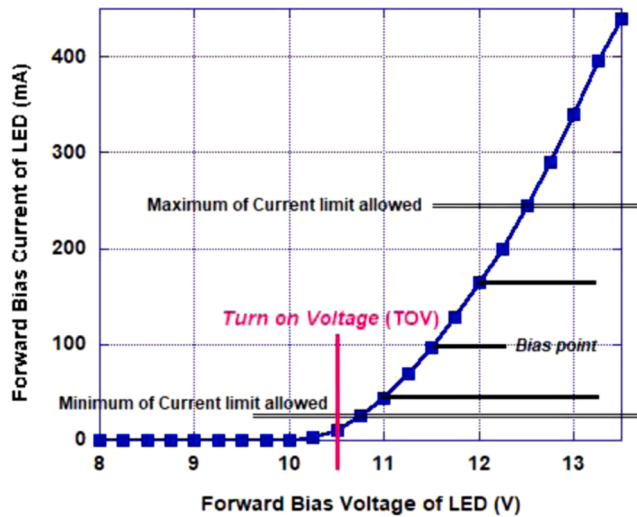


Fig. 8. I-V curve characteristics of the 12 V<sub>DC</sub> LED of CREE XT-E.

Therefore, this work aimed to evaluate BER and explore the maximum data transmission speed attained by the VLC system with the LED driver. QPSK modulation was used to evaluate the linear driver circuit by viewing from BER parameter [14]. Furthermore, this study discussed the specifications of Op-Amps and LEDs and tested the bandwidth and functional simulation using a virtual simulator. Blue LEDs were used, making the driver settings different due to the varied linear areas.

## 2. Design method

### 2.1. Component specification (Op-Amp & LED)

This study used an Op-Amp component released from Texas Instruments. Inc. The manufacturer provides free SPICE® models or files with.mod extension for the most of their components. The downloaded file is run into a SPICE® simulation, and the designer selects Op-Amp which matches the LED driver specifications for VLC applications. The general Op-Amp TL072 is used for LED driver applications because it works in the ± 12 V<sub>DC</sub> voltage range. The bandwidth of TL072 reaches up to 1 MHz with the gain-bandwidth product (GBW) = 3 MHz. Therefore, IC TL072 is quite appropriate for the BW supply target of 500 kHz and is available in the local electronics market at an affordable price. This Typical Op-Amp is also consistent with the design that requires a minimum supply voltage of 5–12 V<sub>DC</sub> as an LED supply with varying power. Table 1 shows the detailed specifications.

This study utilized an LED with a voltage of 12 V<sub>DC</sub> (power = 8 Watt) produced by CREE.Inc, the XT-E type with blue color ( $\lambda = 465\text{--}480$  nm). LED XT-E has a beam angle = 120° and BW = 1 MHz. Fig. 7 shows the LED's physical appearance.

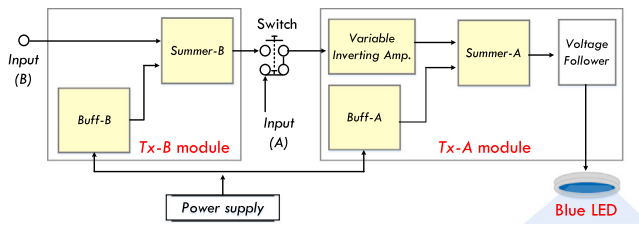
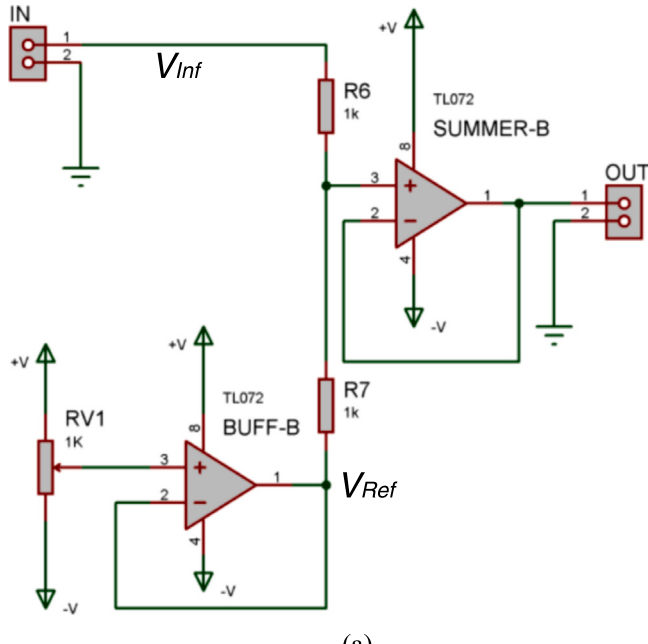
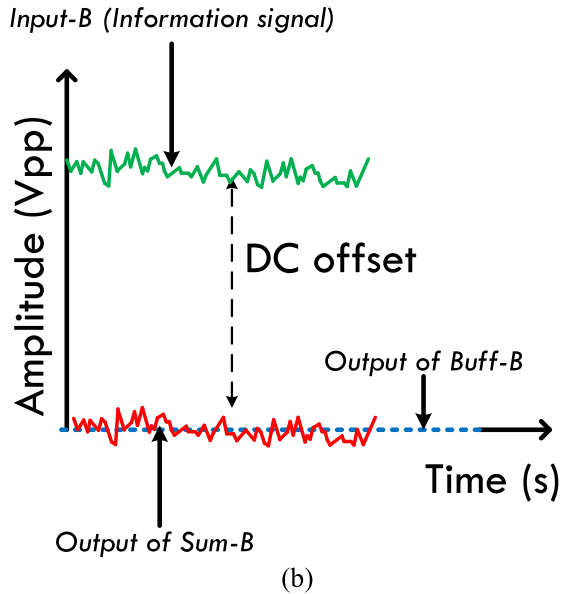


Fig. 9. Block diagram of linear LED driver circuit.



(a)



(b)

Fig. 10. LED driver circuit for input signal characteristics that have DC-offset: (a) Tx-B circuit consisting of a buffer configuration and negative summing amplifier; (b) illustration of how the Tx-B circuit works.

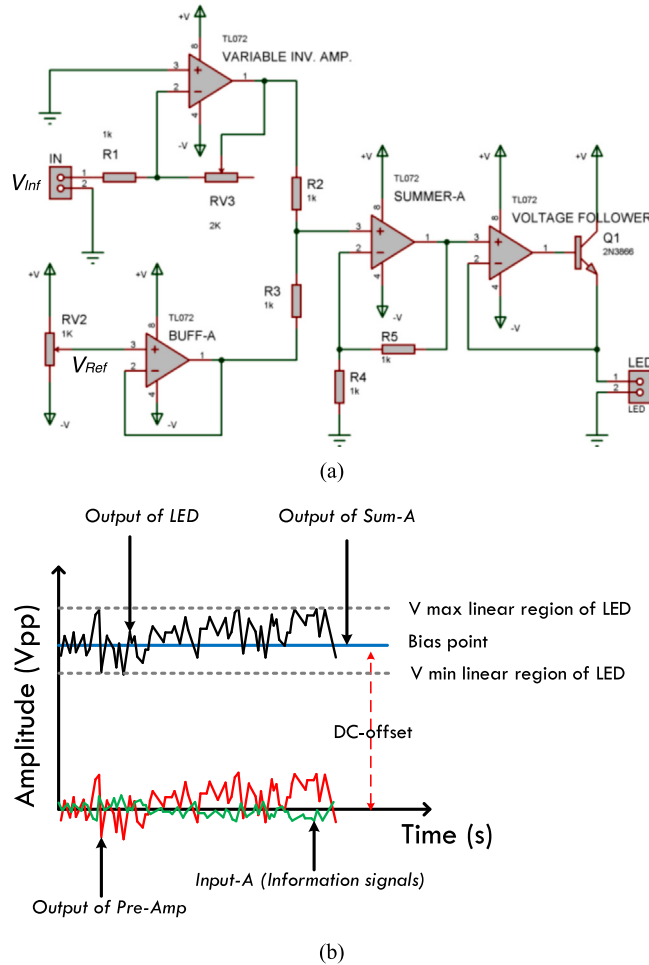


**Fig. 11.** LED driver circuit for input signal characteristics that do not have DC offset: (a) Tx-A circuit consisting of buffer configuration and summing amplifier; (b) illustration of how the Tx-A circuit works.

## 2.2. I-V curve of the LED

The first stage in designing a linear LED driver is determining the forward bias voltage ( $V_f$ ) curve with the current ( $i_f$ ) of the driver used. According to [10], the relationship between  $V_f$  and  $i_f$  is found in the LED datasheet or its characterization. This study characterized the  $V_f$  curve against  $i_f$  of the XT-E LED to determine the curve in real operating conditions, as shown in Fig. 8. The linear working area for the recommended 8-Watt blue LED is in the voltage range of 11–12 V<sub>DC</sub> (LED linear area = ~1 V<sub>DC</sub>, bias point = 11.5 V<sub>DC</sub>). Therefore, the information signal from the Digital Signal Processing (DSP) module or generator must be conditioned at an amplitude of 1 V<sub>DC</sub> by the linear LED driver.

## 2.3. Anatomy of linear LED driver

The LED driver design is composed of the Tx-A module that takes the input signals without DC-offset and Tx-B connected to Tx-A for input signal characteristics with DC-offset. Fig. 9 shows details of the proposed linear LED driver block diagram. The naming of this LED driver module referred to the previous study [15].

The Tx-B module is a DC-offset remover circuit with two Op-Amp configurations, a buffer, and a negative summing amplifier. When the input signal composed of DC offsets, such as Digital to Analog Converter (DAC), or THS651EVM module, is amplified without removal, the DC signal is also amplified, causing incorrect LED bias-point settings. Fig. 10(a) shows the configuration of the Tx-B module, while Fig. 10(b) illustrates how the circuit works. The DC-offset value is regulated by the potentiometer RV1 on Buff-B, which should be conditioned to meet:  $V_{Ref} = 0$  V<sub>DC</sub>, where the  $V_{Ref}$  voltage is the reference voltage. This means that the DC signal is kept at 0 V<sub>DC</sub> level, and the information on the touching position to the negative saturation voltage is  $-V_{DC}$ . There is no amplification on the Tx-B module because the output signal from Sum-B, a summing amplifier module, is processed in the variable inverting amplifier on the Tx-A module. The transfer function is given in Eq. (1).

The value of  $R_6$  and  $R_7$  is chosen as 1 k $\Omega$ , when  $V_{ref} = 0$  V, Eq. (1) is rewritten into Eq. (2), where  $V_{in}$  of the DAC board = 1 V<sub>DC</sub>.

$$V_{SUM-B} = \left( \frac{R6}{R6 + R7} V_{in} + \frac{R7}{R6 + R7} V_{ref} \right) \quad (1)$$

$$V_{SUM-B} = 0,5 * V_{in} \quad (2)$$

The Tx-A module is a DC-offset adder circuit composed of the variable inverting and summing amplifiers, buffer, and voltage follower transistor. The DC signal from the DAC board has been removed, leaving only the information signal. Furthermore, the signal should be adjusted to the linear region of the LED used. The settings are made in the variable inverting amplifier block. The inverting port is selected in amplifier configuration for attaining the signal attenuation. This is different from the non-inverting amplifier, which has 1 gain, meaning gain = 1 + ( $R_f/R_g$ ). The LED is turned on by coupling the information with a DC-offset signal by a summing amplifier, making it also carry information based on intensity modulation direct detection (IM/DD). Fig. 11(a) shows the configuration of the Tx-A module, while Fig. 11(b) illustrates the circuit working principle. Eq. (3) is used to calculate the gain in the amplifier module with a fixed  $R_f$ . The resistor value in the Tx-A module is made as a variable, where  $RV3 = 2$  k $\Omega$  and  $R_g = 1$  k $\Omega$ .

$$Gain_{amp} = -\frac{Rf}{Rg} = -\frac{RV3}{Rg} \quad (3)$$

The resulting signal from the gain for the minimum  $RV3$  condition is:

$$\text{Maximum Gain of amp.} = -\frac{2 \text{ k}\Omega}{1 \text{ k}\Omega} = 2 \text{ times}$$

And the gain for the maximum  $RV3$  condition is

$$\text{Minimum Gain of amp.} = -\frac{0.5 \text{ k}\Omega}{1 \text{ k}\Omega} = 0.5 \text{ times}$$

The results showed that the gain of the variable inverting amplifier module ranges between 0.5 and 2 times. The output voltage is set to at least 0.5 V<sub>DC</sub> and -0.5 V<sub>DC</sub>, where the V<sub>DC</sub> linear range of the 8 Watts CREE XT-E LED is 1 V<sub>DC</sub>. For instance, amplification is required twice when the input signal is 0.5 VDC. An input signal of 2 V<sub>DC</sub> needs to be attenuated by half.

Potentiometer  $RV2$  is a DC-offset level regulator, while Buff-A is a buffer configuration that maintains the input signal. The next circuit is a summing amplifier (summer-A or Sum-A), which adds the output signals from Buff-A and the variable inverting amplifier. Eq. (4) shows the transfer function of the Sum-A circuit.

$$V_{SUM-A} = \left( \frac{R2}{R2 + R3} V_{in} + \frac{R3}{R2 + R3} V_{ref} \right) * \left( 1 + \frac{R5}{R4} \right) \quad (4)$$

The values of  $R_2$ ,  $R_3$ , and  $R_4$  are chosen as 1 k $\Omega$ , where Eq. (4) is rewritten as Eq. (5).

$$V_{SUM-A} = (0,5 * V_{in} + 0,5 * V_{ref}) * \left( 1 + \frac{1k\Omega}{R4} \right) \quad (5)$$

The previous input signal's peak-to-peak ( $V_{pp}$ ) voltage is 0.5 to -0.5 V<sub>DC</sub>. Therefore, the voltage on the LED in linear conditions is 11–12 V<sub>DC</sub> or in the range of 1 V<sub>DC</sub>, indicating one-time amplification. In Eq. (5), the input signal has been amplified half times obtained from equation = 0.5 ×  $V_{in}$ , meaning the information signal has weakened by 0.5 times. It should be amplified twice to remain at a voltage of 1 V<sub>DC</sub>. Additionally, the DC reference voltage gains by half, derived from the equation = 0.5 ×  $V_{ref}$ . The value of the resistor  $R_4$  is calculated as follows:

$$\left( 1 + \frac{R5}{R4} \right) = 2 \text{ times}, \text{ if } R5 = 1 \text{ k}\Omega \text{ then } R4 = 1 \text{ k}\Omega$$

The last circuit is a voltage follower transistor connected to the LED. The output voltage follows the input voltage of the Sum-A circuit, as explained in Eqs. (6), (7), and (8). The transistor used in this study is a 2N3866 from Motorola, Inc ( $I_c = 1$  Ampere,  $V_c = 28$  V<sub>DC</sub>, 400 MHz). VLED is the maximum linear voltage. To supply the CREE XT-E LED, the min  $V_{ref\ min}$  setting must be positioned at 11 V<sub>DC</sub>, and  $V_{ref\ max} = 11.5$  V<sub>DC</sub>.

$$V_{SUMMER-A} = V_{LED} \quad (6)$$

$$V_{LED} = (0,5 * V_{in} + 0,5 * V_{ref}) * (2) \quad (7)$$

$$V_{LED} = (1 * V_{in} + 1 * V_{ref}) \quad (8)$$

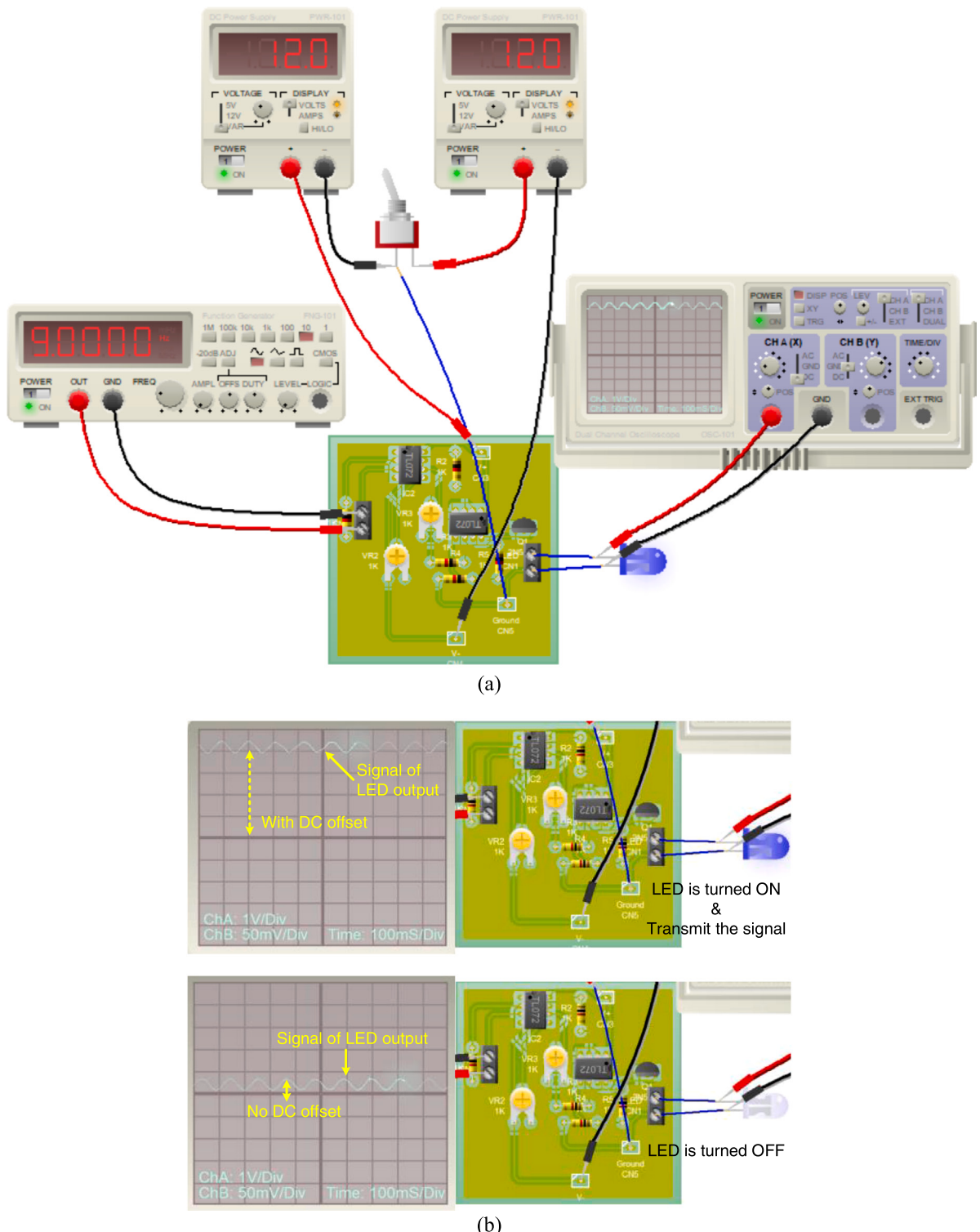


**Fig. 12.** LED driver simulation: (a) circuit simulation; (b) signal capture on a virtual oscilloscope on MULTISIM V.14 comparing the input signal with the LED anode (single carrier signal = sinusoid, amplitude = 0.5 Vpp, input frequency = 5 Hz).

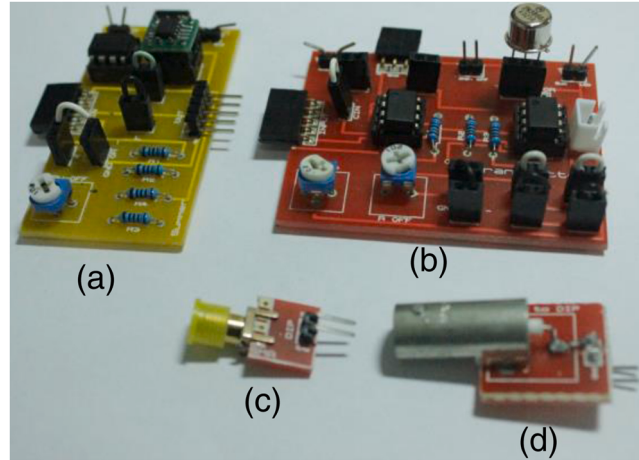


**Fig. 13.** Photo of the linear LED driver prototype made per module: (a) Tx-B module with dimensions of 33.32 mm × 62.56 mm; (b) Module Tx-A = 49.96 mm × 61.85 mm; (c) SMA male connector; (d) BNC male connector.

### 3. Result and discussion

#### 3.1. Linear LED driver simulation

A number of simulations were performed to determine the design's accomplishments before being tested on the project board and fabricated on the PCB for further investigation. In our previous work, we used MULTISIM to conduct a functional circuit analysis of the proposed LED driver design. In contrast, this study uses the Circuit Wizard® trial version software set in virtual mode. The software analyzes the success of simple circuit design, such as the LED driver. It is an interactive GUI demonstrating work like real instruments, components, and contains virtual measuring instruments such as oscilloscopes, signal generators, and multimeters. Additionally, the software provides a large selection of Op-amps from various vendors, including TL072. The simulation circuit is first made in circuit mode and converted into an automatically routed PCB. Circuit Wizard® only provides asymmetric Power Supply. Therefore, to have three channels (i.e., ground, V+, and V-), it should be used two units of asymmetric Power Supply and arranged properly. The Symmetric Power Supply, Frequency Generator, analog Oscilloscope, and blue LED are connected to the PCB, as shown in Fig. 12(a). In this simulation, 2N3866 was replaced by 2N5088. We used 12 V<sub>DC</sub> to supply LED and Op-amps.

A sinusoidal signal with 0.5 V<sub>pp</sub> is generated from the frequency generator at 5 Hz for the sine signal to be seen properly on the Oscilloscope. A higher frequency enables the Circuit Wizard® to display stacked signals. This is based on previous experiments, where the Oscilloscope in the Circuit Wizard® displayed a good sinusoidal signal at frequencies below 1 kHz. The LED driver is expected to be used up to 500 kHz. The value V<sub>ref</sub> should be adjusted to add DC signal on the input signal via Trimpot (V<sub>R2</sub>). The simulation results in Fig. 12(b) show that the LED turns on and transmits data as a sinusoidal signal.

#### 3.2. Implementation and experimental results

A PCB (Printed Circuit Board) prototype of a linear LED driver circuit is shown in Fig. 13(a) and (b) for Tx-A and Tx-B, respectively. The Tx-A and Tx-B modules are made separately, plugged in, and play according to the characteristics of the input signal. The three power input channels of the Tx-A module are V<sub>CC</sub>, ground, and V<sub>EE</sub>, while the Tx-B has five channels, including V<sub>CC</sub>, ground, V<sub>EE</sub>, data, and ground. The output ports on the DAC board use SMA (SubMiniature version A) or BNC (Bayonet Neill-Concelman) connectors. Therefore, this study also made DIP to BNC and DIP to SMA converters. The linear LED driver module was made with Proteus 7.0 Student version software in a double layer PCB using discrete components.

#### 3.3. TL072 Op-Amp bandwidth test

An LED driver circuit with a BW 500 kHz is designed by ensuring the capabilities of the selected components are well comprehended. It is necessary to know the maximum frequency limit passed by the Op-Amp TL072. In this work, observations were made at the amplitude of the input and output signals in the time domain and calculated by Eq. (9). BW is the difference between the highest and lowest frequency within a certain range, as expressed in Eq. (10).

$$20 * \log \frac{V_o}{V_i} \quad (9)$$

$$BW = m_{\text{maximum}} - m_{\text{minimum}} \quad (10)$$

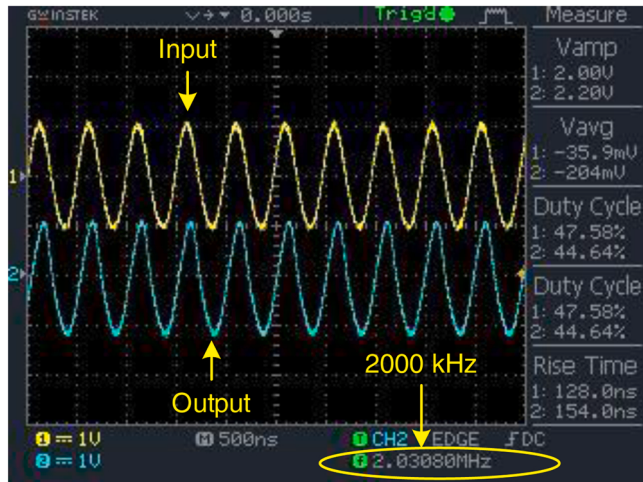


**Fig. 14.** Op-Amp IC performance by using a non-inverting amplifier 1 times amplification on IC TL072 with the frequency of 2 MHz.

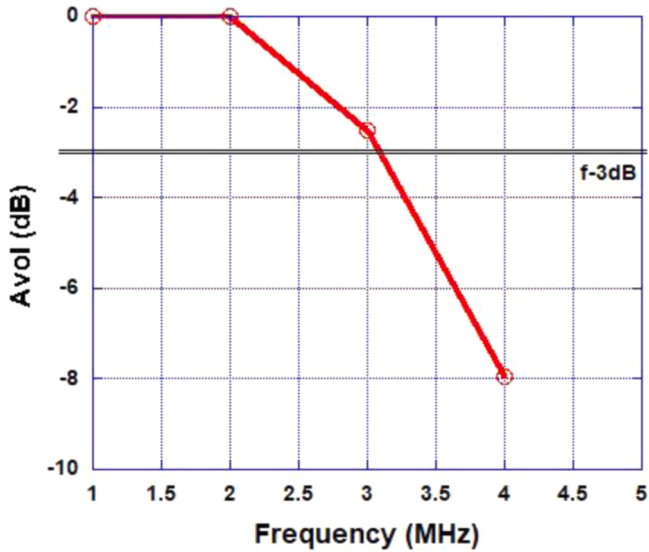


**Fig. 15.** Frequency graph against  $A_{VOL}$  on Op-Amp TL072,  $f_c = 3$  MHz.

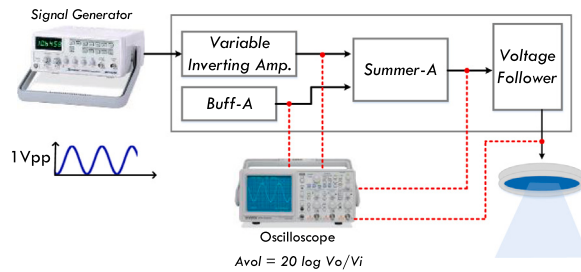


**Fig. 16.** The maximum BW characterization scenario of the Tx-A linear LED driver circuit using a single carrier signal from the signal generator as input.

The input signal comes from a generator (GW-INSTEK GFG-8210) with a frequency varying from 1 MHz to 5 MHz. The signal is sinusoidal, the gain of the non-inverting amplifier = 1, and the input signal amplitude = 2 Vpp. Moreover, this study uses a dual power supply (5 VDC, ground, -5 VDC). **Fig. 14** is an oscilloscope signal capture (GW-INSTEK GDS-1152-AU), where the input and output

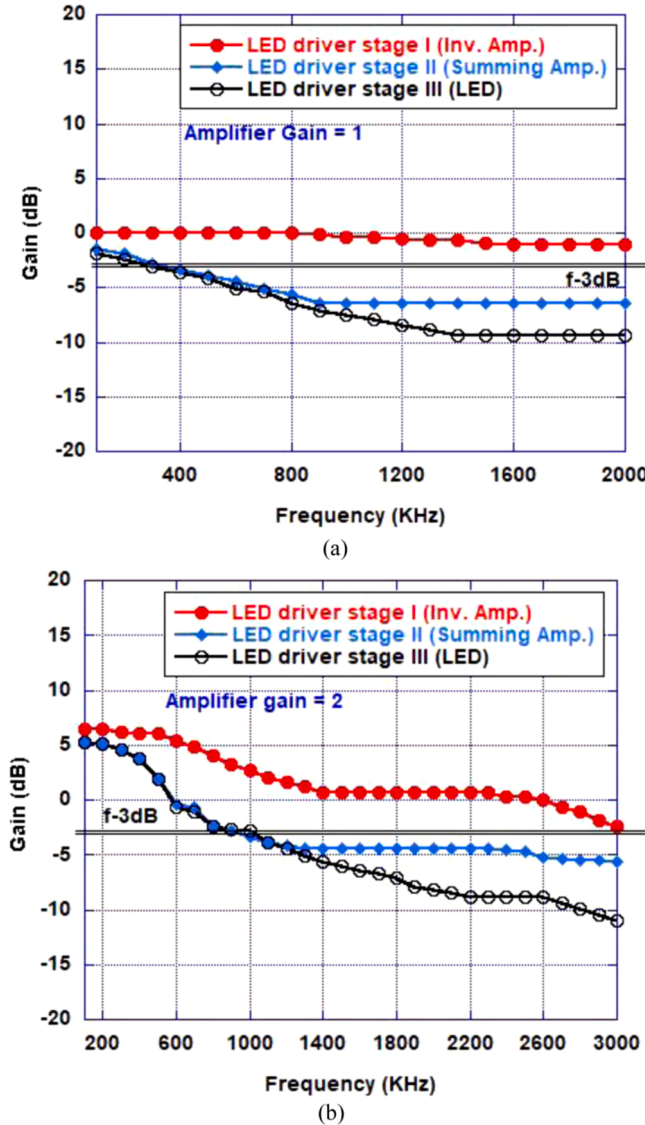


**Fig. 17.** AVOL of each stage in the linear LED driver circuit: (a)  $V_{in} = 1 \text{ V}_{pp}$ , gain = 1x, Maximum effective BW is 400 kHz; (b)  $V_{in} = 1 \text{ V}_{pp}$ , gain = 2x, Effective BW become 1 MHz.

signals are shown in yellow and blue colors, respectively. The amplitude of the output and input signals are the same at 2 MHz. Fig. 15 illustrates the relationship between voltage gain ( $A_{VOL}$ ) and frequency on the Op-Amp TL072, resulting in IC TL072 with a BW of 3 MHz.

#### 3.4. Frequency response of linear LED driver circuit

After designing and implementing the hardware, the next step is to determine the maximum BW of the Tx-A LED driver circuit to determine the optimum frequency transmitted by a linear LED driver circuit. The test procedure is shown in Fig. 16. The parameters used are the input signal from the generator with an amplitude of 1 V<sub>pp</sub>, no DC offset, and a frequency ranging from 100 kHz to 3 MHz.

Fig. 17 shows the graph of the relationship between  $A_{VOL}$  and the frequency of each stage. It shows that stage I is a pre-amp, stage II is a summing amplifier, and stage III is a voltage follower transistor circuit. This test showed that when the pre-amp circuit in the driver uses a gain of 2 times, the  $f_{-3\text{ dB}}$  or  $f_c$  increases to 1 MHz. A higher frequency attenuates the voltage follower transistor circuit due to the LED's parasitic capacitance effect [24] that reduces BW. Additionally, a higher input frequency exceeding the BW increases the capacitance and reduces the  $A_{VOL}$ , dimming the LED [25].

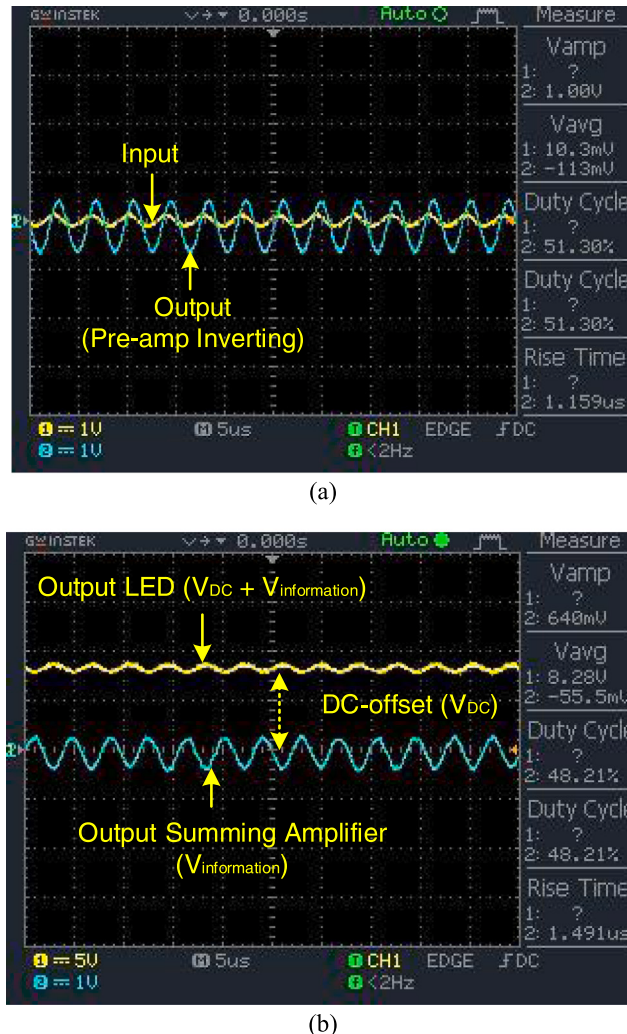


**Fig. 18.** Functionality test of LED driver circuit: (a) input signal (yellow) vs. output of pre-amp inverting amplifier circuit (blue); (b) output from summing amplifier (blue) vs. LED (yellow).

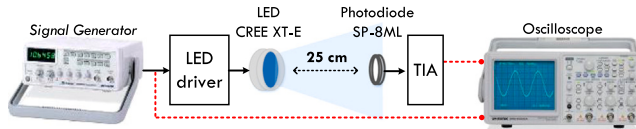
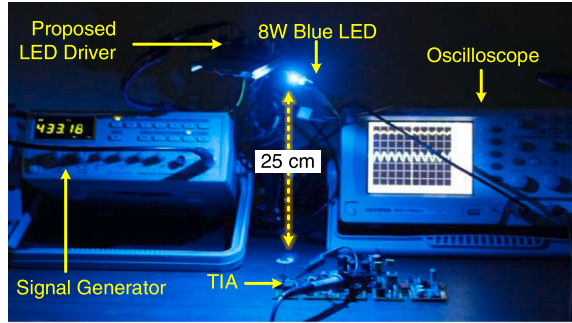


**Fig. 19.** Test bench of LED driver linear (single carrier signal).

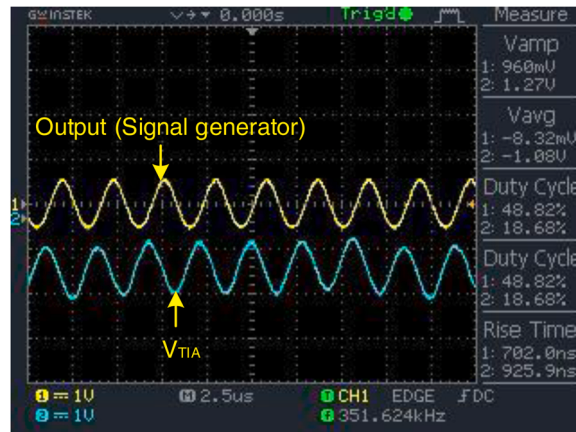
### 3.5. Functional test of linear LED driver with a sinusoidal signal (single carrier signal)

Fig. 16 shows the functional test setup of a linear LED driver using a single carrier signal as the input. The signal generator was set to an amplitude of  $0.5 \text{ V}_{\text{pp}}$  and connected to the input block of the variable inverting amplifier. Additionally, the signal processing in the linear LED driver circuit was observed using an oscilloscope.

Fig. 18(a) is the original signal from the generator and the output of the variable non-inverting amplifier circuit. The results show that the input signal is amplified and adjusted manually using a potentiometer to the maximum limit of the LED by  $1 \text{ V}_{\text{pp}}$ .  $V_{\text{offset}}$  should add the amplified signal from the power supply to light the LED from the Turn-on-voltage (TOV) condition range to the maximum limit of the  $V_{\text{max}}$  by the summing amplifier circuit block.  $V_{\text{LED}}$  is the sum of the sinusoidal or information and the DC signals, as shown in Fig. 18(b). The output signal from the summing amplifier was shifted to position  $0 \text{ V}_{\text{pp}}$ , and  $V_{\text{LED}}$  was multiplied by the  $5 \text{ V}_{\text{pp}}$  scale. Consequently, the linear LED driver design works similar to a T-bias module shown in Fig. 5(b)), with  $V_{\text{LED}}$



**Fig. 20.** A photograph of a Test bench linear LED driver using a single-carrier signal.



**Fig. 21.** Functionality test of single-carrier signal transmission, the input signal is shown in yellow, and V<sub>TIA</sub> is shown in blue.

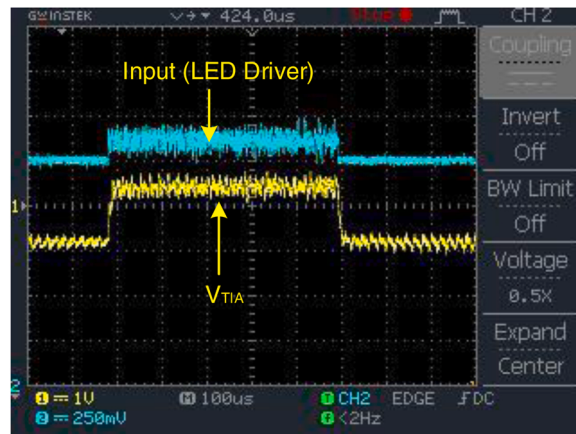


**Fig. 22.** Functionality test of multicarrier signal transmission with multilevel amplitude format; input signal is indicated in yellow, and VTIA is indicated in blue.

$= V_{\text{information}} + V_{\text{DC}}$ , as shown in Fig. 18(b). This driver could replace the Bias-T module by offering an economical advantage.

The next stage was testing the transmission of a single carrier signal through an optical channel. The experimental setup is shown in Fig. 19, while the laboratory test photo is indicated in Fig. 20. The input signal is a sinusoidal which is generated from a generator and transmitted by the CREE XT-E LED. The Kodensi SP-8ML PIN photodiode on the receiver side captures and converts the optical signal into the current. The TIA circuit is used to convert the current into voltage (V<sub>TIA</sub>). Therefore, the input signal from the linear driver LED and V<sub>TIA</sub> is observed not through the oscilloscope. The channel distance is 25 cm, the input frequency is 350 kHz, and the LED is perpendicular to the photodiode.

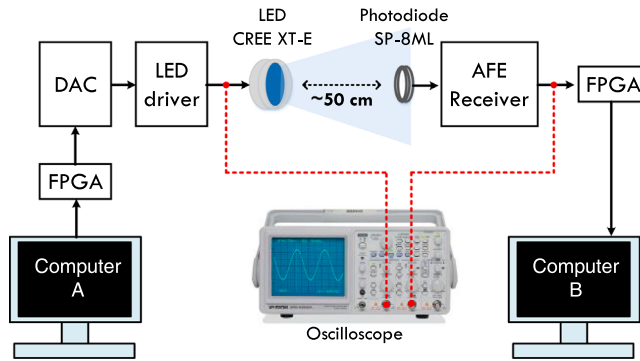


**Fig. 23.** Experimental setup for a real-time test containing proposed LED driver, DAC board, and FPGA transceiver.

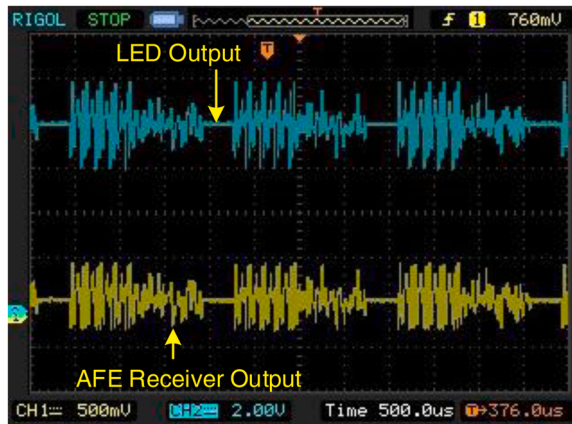


**Fig. 24.** OFDM signal on LED output and receiver AFE output.

```
root@localhost:~/Documents/workspace/vlc-linux-tx
root@localhost:~/Documents/workspace/vlc-linux-tx# ./vlc-linux-tx
Lorem ipsum dolor sit amet, consectetur adipiscing elit. Vivamus dolor nulla, malesuada vel metus eget, egestas consectetur risus. Maecenas turpis ipsum, tristique eget volutpat id, venenatis a lectus. Nunc ac hendrerit metus. Nullam lorem quam, interdum sit amet gravida in, tempor vel metus. Morbi velit neque, tincidunt et magna eu, mattis imperdiet purus. Cras facilisis felis sed molestie lacinia. Quisque augue eros, tempus eu hendrerit sed, feugiat in libero. In hac habitasse platea dictumst. In sed luctus dolor. Ut tortor mi, rhoncus sed molestie at, volutpat vitae eros. Quisque faucibus tortor ut bibendum imperdiet. Vivamus purus orci, elementum eu ornare at, convallis in orci. Fusce eleifend, sapien at interdum pretium, dolor dolor tristique urna, eget eleifend augue orci non lorem. Curabitur et posuere risus.

Vestibulum mollis condimentum ex, quis maximus lorem viverra eu. Aliquam scelerisque facilisis orci a tincidunt. Maecenas aliquam, lectus et luctus imperdiet, tortor felis malesuada dui, id aliquam massa purus sit amet
root@localhost:~/Documents/workspace/vlc-linux-tx#
```

**Fig. 25.** Program log on ZYBO transmitter.

**Fig. 21** compares the input signals from the LED driver circuit to the V<sub>TIA</sub>. The observation results showed that the sinusoidal signal transmitted by the LED is well received by the TIA circuit, this translates that the driver works perfectly. BW measurement from integrating the transmitter and receiver circuits is out of the scope of this work, we limited our study to functional experiments.

A functionality test was conducted with an input containing DC offset and characteristic multilevel amplitude of DAC module (THS651EVM) from Analog Devices. Inc. Previous studies verified the functionality of the DAC module [26]. Although the experimental setup refers to **Fig. 19**, the linear LED driver circuit was connected to the DAC module, the DSP FPGA device, and the personal computer (PC) at the input. The transmitted information is a multicarrier OFDM signal. The experimental results are presented in **Fig. 22** that the OFDM signal is transmitted by the linear driver LED without flicker and received by TIA with no DC offset.

ls  
lorem-ipsum.txt vlc-linux-rx vlc-linux-rx.c  
root@localhost:~/Documents/workspace/vlc-linux-rx#  
root@localhost:~/Documents/workspace/vlc-linux-rx# ./vlc-linux-rx  
Lorem ipsum dolor sit amet, consectetur adipisciing elit. Vivamus  
dolor nulla, malesuada vel metus eget, egestas consectetur risus.  
Maecenas turpis ipsum, tristique eget volutpat id, venenatis a  
lectus. Nunc ac hendrerit metus. Nullam lorem quam, interdum sit  
amet gravida in, tempor vel metus. Morbi velit neque, tincidunt et  
magna eu, mattis imperdiet purus. Cras facilisis felis sed  
molestie lacinia. Quisque augue eros, tempus eu hendrerit sed,  
feugiat in libero. In hac habitasse platea dictumst. In sed luctus  
dolor. Ut tortor mi, rhoncus sed molestie at, volutpat vitae eros.  
Quisque faucibus tortor ut bibendum imperdiet. Vivamus purus orci,  
elementum eu ornare at, convallis in orci. Fusce eleifend, sapien  
at interdum pretium, dolor dolor tristique urna, eget eleifend  
augue orci non lorem. Curabitur et posuere risus.  
  
Vestibulum mollis condimentum ex, quis maximus lorem viverra eu.  
Aliquam scelerisque facilisis orci a tincidunt. Maecenas aliquam,  
lectus et luctus imperdiet, tortor felis malesuada dui, id aliquam  
massa purus sit amet  
Total bit error: 0, Total: 8400  
root@localhost:~/Documents/workspace/vlc-linux-rx#  
root@localhost:~/Documents/workspace/vlc-linux-rx# |

**Texts comparison**

Fig. 26. Program log on ZYBO receiver.

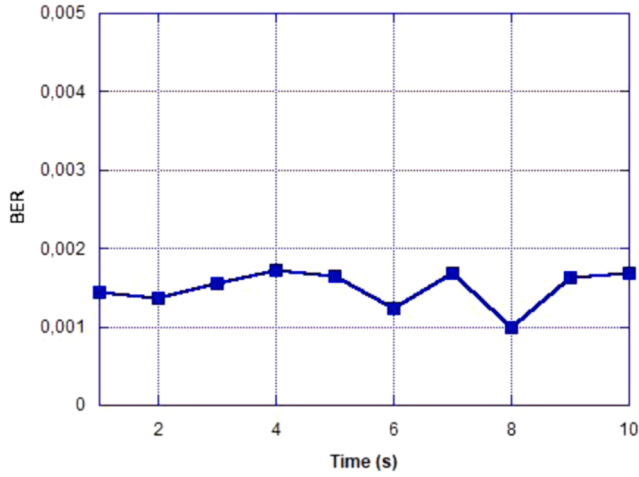


Fig. 27. BER Testing.

### 3.6. Real-time VLC system demonstration with QPSK Modulation

Fig. 23 is a linear LED driver test setup with real-time VLC architecture, where the DSP platform utilizes other studies [14,23,27, 28]. This test exploited two FPGA (ZYBO board) as transmitter and receiver, respectively, an 8-bit DAC (Analog Devices AD7302) module with a voltage range of 3.3 V<sub>DC</sub>, and an AFE receiver module composed of TIA, Preamp, and Filter, separate from this study [8]. Furthermore, the experiment uses the ADC available on the Zynq-7000 FPGA, a 12-bit XADC with a voltage of 1 V<sub>DC</sub>. The FPGA

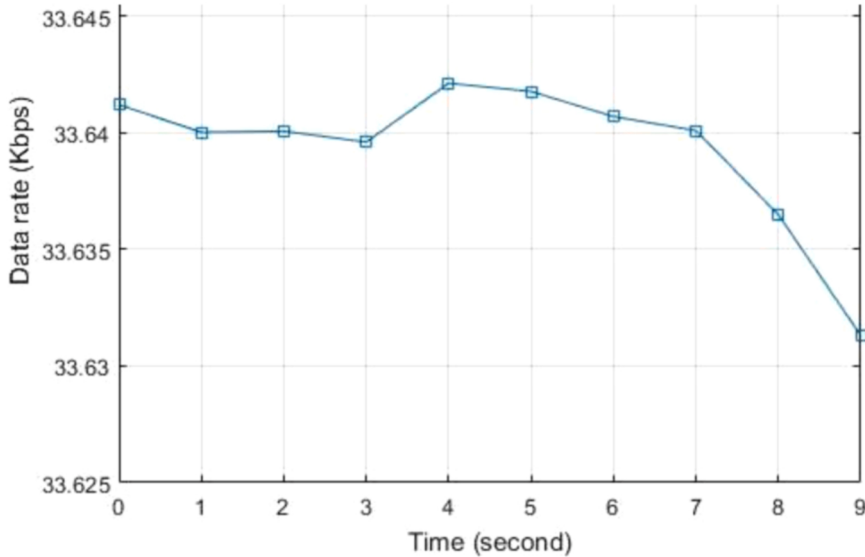


Fig. 28. Data transmission speed test (QPSK modulation).

transmitter module was connected to the input of the AD7302 DAC, and the DAC output was fed to the proposed Linear LED driver's input. The FPGA ADC pin was connected to the receiver's AFE output, while the optical channel distance was about 50 cm. The sampling rate between the DAC and ADC was set at 100 kHz, 10 times lower than the available linear driver LED bandwidth. Additionally, two-channel Oscilloscopes were connected to the LED output and AFE receiver for comparison.

Fig. 24 shows the observation result of the QPSK modulated OFDM signal at the LED output (blue) and the AFE receiver output (AFE receiver). The signal contains Time offset, Cyclic prefix + Preamble, Cyclic Prefix + data, and Guard Interval [14,29]. The received signal is identical to the signal emitted by the LED but needs further verification. A program on the Linux operating system was created before BER and data rate testing. The program allows the platform to send and receive text data from the transmitter for further comparison. Therefore, the text parameters of the transmitter and receiver were compared, and the error bits were counted using the QPSK modulation. Figs. 25 and 26 are the logs of the transmitter program while sending text 1050 bytes in size and the ZYBO receiver's log results, respectively. The comparison shows that all data were successfully received with 0-bit errors out of 8400 bits sent. BER test was performed by sending stream random bit data continuously 10 times. The sent and received stream bit data were compared, and the number of different bits was calculated. The results showed that the developed linear LED driver achieved a real-time VLC system with an average BER of  $1.49 \times 10^{-3}$  (Fig. 27).

A test was performed on the data transfer speed obtained using a sampling clock of 100 kHz. Stream random bit data of 10500 bytes with a 1-second interval was sent from the FPGA transmitter to the FPGA receiver via the optical channel ( $\sim 50$  cm). The delivery time was measured using a timer on the Linux OS, while the speed achieved was 33.6 kbps (with QPSK). This data rate was increased by increasing the clock rate on the FPGA to exceed 100 kHz. However, what was considered consideration is the LED driver's ability, which is a maximum of 1 MHz. Finally, this work confirms the study of [30] that the off-the-shelf LED driver is lower performance than original Bias-T module in terms of data rate, but it is more inexpensive. Fig. 28.

In summary, a linear LED driver module for VLC applications has been proposed and carefully evaluated. The driver module contains a DC-offset remover that is used for the input signal and a DC-offset adder to add the information signal. The two components enable the driver to light while positioning the information signal in the linear region. The designed driver compensates for LED's nonlinear problem, emitting a multilevel amplitude similar to an OFDM or an original analog-based audio and video information signal. The validity of the proposed method has been performed through simulations and experiments and paved the way to implement such driver modules in low-data rate VLC applications.

#### 4. Conclusions and future work

This study aimed to design and implement a linear LED driver module composed of the DC-offset Remover utilized for the input signal and a DC-offset Adder to add an information signal. The two components enable the driver to light while positioning the information signal in the linear region. The designed driver compensates for LED's nonlinear problem, emitting a multilevel amplitude similar to an OFDM or an original analog-based audio and video information signal. Functionality tests showed that the linear LED driver could replace a commercial Bias-T module with a BW capacity of 500 kHz and a maximum of 1 MHz. Additionally, it was tested on a real VLC system with a QPSK modulation and obtained  $1.495 \times 10^{-3}$  average BER. This linear LED driver's maximum data transfer speed is 33.6 kbps, with a clock speed of 100 kHz on the FPGA. The further study of hardware implementation in terms of bandwidth and video transmission is a subject of future work.

## Declaration of Competing Interest

The authors declare that they have no known competing financial interests or personal relationships that could have appeared to influence the work reported in this paper.

## Data availability

No data was used for the research described in the article.

## Acknowledgements

The authors would like to acknowledge to Universitas Pendidikan Indonesia (UPI) for funding this work through the Indonesian Collaboration Research – World Class University (Riset Kolaborasi Indonesia/RKI – WCU) Grant in 2022 with Contract No. 1165/UN40.LP/PT.01.03/2022 in conjunction with Penelitian Penguatan Kompetensi scheme in 2022 with Contract No. 805/UN40.LP/PT.01.03/2022.

## References

- [1] T. Komine, M. Nakagawa, Fundamental analysis for visible-light communication system using LED lights, *IEEE Trans. Consum. Electron.* vol. 50 (1) (2004) 100–107, <https://doi.org/10.1109/TCE.2004.1277847>.
- [2] H. Elgala, R. Mesleh, H. Haas, Indoor optical wireless communication: potential and state-of-the-art, *IEEE Commun. Mag.* vol. 49 (9) (2011) 56–62, <https://doi.org/10.1109/MCOM.2011.6011734>.
- [3] S. Fuada, A.P. Putra, T. Adiono, Analysis of received power characteristics of commercial photodiodes in indoor los channel visible light communication, *Int. J. Adv. Comput. Sci. Appl. (IJACSA)* vol. 8 (7) (2017), <https://doi.org/10.14569/IJACSA.2017.080722>.
- [4] S. Fuada, Kajian Aspek Security pada Jaringan Informasi dan Komunikasi Berbasis Visible Light Communication, *INFOTEL* vol. 9 (1) (2017) 108–121, <https://doi.org/10.20895/infotel.v9i1.163>.
- [5] T. Adiono, S. Fuada, S. Harimurti, Bandwidth Budget Analysis for Visible Light Communication Systems utilizing Commercially Available Components, in *Proceedings the 10th International Conference on Electrical and Electronics Engineering (ELECO)*, Bursa, Turkey, 2017, pp. 1375–1380.
- [6] S. Fuada, T. Adiono, Rancang Bangun Layer Fisik Visible Light Communication Pada Sistem Transmisi Audio, *J. INFOTEL* vol. 9 (3) (2017) 352–360, <https://doi.org/10.20895/infotel.v9i3.288>.
- [7] A.R. Ndjiougue, H.C. Ferreira, T.M.N. Ngatchatché, Visible Light Communications (VLC) Technology. Wiley Encyclopedia of Electrical and Electronics Engineering, John Wiley & Sons, Ltd, 2015, pp. 1–15, <https://doi.org/10.1002/047134608X.W8267>.
- [8] Syifaul Fuada, Design and Implementation of Analog Front-End Transceiver Module for Visible Light Communication System, Master Thesis, Department of Electrical Engineering, School of Electrical Engineering and Informatics (SEEI), Bandung, Indonesia, 2017.
- [9] T. Adiono, S. Fuada, A.P. Putra, Y. Aska, Desain awal analog front-end optical transceiver untuk aplikasi visible light communication, *J. Nas. Tek. Elektro Dan. Teknol. Inf. (JNTETI)* vol. 5 (4) (2016) 319–327, <https://doi.org/10.22146/jnteti.v5i4.280>.
- [10] H. Elgala, R. Mesleh, H. Haas, An LED model for intensity-modulated optical communication systems, *IEEE Photonics Technol. Lett.* vol. 22 (11) (2010) 835–837, <https://doi.org/10.1109/LPT.2010.2046157>.
- [11] M.R. Luo, F. Zhao, Q. Zhai, X. Liu, B. Wang, The impact of LED on human visual experience, in *2013 10th China International Forum on Solid State Lighting (ChinaSSL)*, Beijing, China, Nov. 2013, pp. 280–283. doi:[10.1109/SSLCHINA.2013.7177370](https://doi.org/10.1109/SSLCHINA.2013.7177370).
- [12] T. Katsuura, Y. Ochiai, T. Senoo, S. Lee, Y. Takahashi, Y. Shimomura, Effects of blue pulsed light on human physiological functions and subjective evaluation, *J. Physiol. Anthropol.* vol. 31 (1) (2012) 23, <https://doi.org/10.1186/1880-6805-31-23>.
- [13] M. Davidovic, L. Djokic, A. Cabarkapa, M. Kostic, Warm white versus neutral white LED street lighting: Pedestrians' impressions, *Light. Res. Technol.* vol. 51 (8) (2019) 1237–1248, <https://doi.org/10.1177/1477153518804296>.
- [14] S. Fuada, E. Setiawan, T. Adiono, W.O. Popoola, Design and verification of SoC for OFDM-based visible light communication transceiver systems and integration with off-the-shelf analog front-end, *Optik* vol. 258 (2022), 168867, <https://doi.org/10.1016/j.jleo.2022.168867>.
- [15] S. Fuada, T. Adiono, A.P. Putra, Y. Aska, LED driver design for indoor lighting and low-rate data transmission purpose, *Optik* vol. 156 (2018) 847–856, <https://doi.org/10.1016/j.jleo.2017.11.180>.
- [16] S. Fuada, T. Adiono, A.P. Putra, Y. Aska, A low-cost Analog Front-End (AFE) transmitter designs for OFDM visible light communications, in *2016 International Symposium on Electronics and Smart Devices (ISESD)*, Bandung, Indonesia, Nov. 2016, pp. 371–375. doi:[10.1109/ISESD.2016.7886750](https://doi.org/10.1109/ISESD.2016.7886750).
- [17] S. Fuada, Prototyping design of low-cost bias-t circuit based-on op-amp for visible light communication, *JCM* vol. 17 (1) (2022) 63–73, <https://doi.org/10.12720/jcm.17.1.63-73>.
- [18] I. Stefan, H. Elgala, R. Mesleh, D. O'Brien, H. Haas, Optical Wireless OFDM System on FPGA: Study of LED Nonlinearity Effects, in *2011 IEEE 73rd Vehicular Technology Conference (VTC Spring)*, Budapest, Hungary, May 2011, pp. 1–5. doi:[10.1109/VETEC.2011.5956691](https://doi.org/10.1109/VETEC.2011.5956691).
- [19] D. Iturralde, A. Abad, I. Cordero, G. Delgado, A. Cabrera, Performance Analysis of the Bias Tee Circuit in Visible Light Communications, in *2020 South American Colloquium on Visible Light Communications (SACVC)*, Santiago, Chile, Jun. 2020, pp. 1–4. doi:[10.1109/SACVLC50805.2020.9129863](https://doi.org/10.1109/SACVLC50805.2020.9129863).
- [20] J.B. Carvalho et al., An ultra low cost Bias Tee unit, in *2011 SBMO/IEEE MTT-S International Microwave and Optoelectronics Conference (IMOC 2011)*, Natal, Brazil, Oct. 2011, pp. 199–202. doi:[10.1109/IMOC.2011.6169264](https://doi.org/10.1109/IMOC.2011.6169264).
- [21] Y.-H. Chang, P.-H. Yang, C.-H. Yeh, C.-W. Chow, Passive 100W High Power Bias-Tee for Visible Light Communication Systems, in *2020 Opto-Electronics and Communications Conference (OECC)*, Taipei, Taiwan, Oct. 2020, pp. 1–3. doi:[10.1109/OECC48412.2020.9273606](https://doi.org/10.1109/OECC48412.2020.9273606).
- [22] C.-S.A. Gong, Y.-C. Lee, J.-L. Lai, C.-H. Yu, L.R. Huang, C.-Y. Yang, The high-efficiency LED driver for visible light communication applications, *Sci. Rep.* vol. 6 (1) (2016) 30991, <https://doi.org/10.1038/srep30991>.
- [23] E. Setiawan, S. Fuada, T. Adiono, Experimental Demonstration of OFDM Visible Light Communications based on System-on-Chip, in *2018 International Symposium on Electronics and Smart Devices (ISESD)*, Bandung, Oct. 2018, pp. 1–5. doi:[10.1109/ISESD.2018.8605466](https://doi.org/10.1109/ISESD.2018.8605466).
- [24] J. Rose, et al., Driving LED in a nanosecond regime by a fast operational amplifier, *arXiv* (2010), <https://doi.org/10.48550/arXiv.1011.1954>.
- [25] P. Deng, M. Kavehrad, Effect of white LED DC-bias on modulation speed for visible light communications. *arXiv* (2016) <https://doi.org/10.48550/arXiv.1612.08477>.
- [26] S. Fuada, A.P. Putra, Y. Aska, A. Pradana, E. Setiawan, T. Adiono, Implementasi Perangkat digital signal processing untuk sistem visible light communication, *Jetri: J. Ilm. Tek. Elektro* vol. 15 (2) (2018) 101–126, <https://doi.org/10.25105/jetri.v15i2.2352>.
- [27] E. Setiawan, T. Adiono, S. Fuada, PHY Layer Design of OFDM-VLC System based on SoC using Reuse Methodology, in *2018 International SoC Design Conference (ISOCC)*, Daegu, Korea (South), Nov. 2018, pp. 115–116. doi:[10.1109/ISOCC.2018.8649904](https://doi.org/10.1109/ISOCC.2018.8649904).

- [28] E. Setiawan, T. Adiono, Design of AXI4-stream based modulator IP core for visible light communication system-on-chip, *J. INFOTEL* vol. 10 (2) (2018) 83–89, <https://doi.org/10.20895/infotel.v10i2.367>.
- [29] E. Setiawan, T. Adiono, S. Fuada, Modelling the OFDM-based PHY layer in SoC for visible light communication, *Int. J. Recent Contrib. Eng., Sci. IT (iJES)* vol. 7 (3) (2019) 79–89.
- [30] H. Huang, et al., Visible-light communication using high-power LED panel-lamp and low-complexity MOSFET circuit, *Opt. Quant. Electron* vol. 53 (1) (2021) 38, <https://doi.org/10.1007/s11082-020-02700-2>.